Structural changes in subdomain 2 of G-actin observed by fluorescence spectroscopy

Joanna MORACZEWSKA*†‡, Hanna STRZELECKA-GOŁASZEWSKA†, Pierre D. J. MOENS* and Cristobal G. DOS REMEDIOS*

*Muscle Research Unit, Department of Anatomy and Histology, and Sydney Institute for Biomedical Research, University of Sydney, Sydney 2006, Australia, and †Department of Muscle Biochemistry, Nencki Institute of Experimental Biology, 3 Pasteur Street, PL-02-093 Warsaw, Poland

The influence of DNase I binding to Ca-ATP-G-actin and of Ca^{2+}/Mg^{2+} and ATP/ADP exchange on the conformation of G-actin were investigated by measuring the fluorescence of dansyl cadaverine (DC) conjugated to Gln^{41} in subdomain 2 of the protein. Fluorescence resonance energy transfer (FRET) between this probe and *N*-[4-(dimethylamino)-3,5-dinitrophenyl]maleimide (DDPM) attached to Cys^{374} in subdomain 1 was also measured. Contrary to an earlier report [dos Remedios, Kiessling and Hambly (1994) in Synchrotron Radiation in the Biosciences (Chance, B., Deisenhofer, J., Ebashi, S., Goodhead, D. T., Helliwell, J. R., Huxley, H. E., Iizuka, T., Kirz, J., Mitsui, T., Rubenstein, E. et al., eds.), pp. 418–425, Oxford University Press, Oxford], the distance between these probes did not change significantly when DNase I was bound to actin. A small but reproducible increase in the quantum yield and a blue shift of the DC fluorescence maximum were observed when bound Ca^{2+} was replaced by Mg^{2+}. A large increase (about 70 %) in the quantum yield and an approx. 12 nm blue shift of the emission spectrum occurred when ATP in Mg-G-actin was replaced by ADP. These changes were not accompanied by any significant change in the FRET distance between the dansyl donor and DDPM acceptor probes. A substantial change in the fluorescence of DC-actin was observed after proteolytic removal of the last three residues of actin, in accordance with earlier evidence suggesting that there is a conformational coupling between subdomain 2 and the C-terminal segment in subdomain 1 of actin. The results are discussed in relation to recently published data obtained with another fluorescent probe and to earlier observations based on limited cleavage using proteolytic enzymes.

INTRODUCTION

Since the report by Kabsch et al. [1] of the atomic structure of the complex of monomeric actin with DNase I, two other laboratories have published the structures of α- and β-actin isoforms complexed with segment 1 of gelsolin [2] and with profilin [3] respectively. In general these structures are very similar, although there are local differences which may be due to different sequences of the actin isoforms as well as to changes induced by the binding of the different proteins used for the co-crystallizations.

Actin contains so-called 'small' and 'large' domains separated by a deep cleft, with the small domain comprising subdomains 1 and 2 and the large domain comprising subdomains 3 and 4. One of the observed differences concerns the structure of the DNase I binding loop (residues 38–52) on the top of subdomain 2. This loop is well defined in the actin–DNase I [1] and the actin–profilin [3] co-crystals, but is not well resolved in those containing gelsolin segment 1 [2], probably because it is disordered or highly mobile. In the profilin–β-actin crystals this region is stabilized by the crystal contacts between adjacent actin monomers and its structure is well resolved [3], but it has a slightly different conformation when compared with the actin–DNase I crystals (see [4] for a review). Another region of structural and functional interest is the C-terminal region. The location of the three C-terminal residues (373–375) in the actin–DNase I complex was modelled because these residues were removed by tryptic digestion before crystallization [1]. Profilin and gelsolin segment 1 bind to the intact C-terminal region, but their binding may alter the structure of this region. Recently we determined the radial co-ordinate of fluorescent probes attached to Cys^{374} in F-actin and showed that they were located at a radius of $(17–18)\pm5$ Å [$(1.7–1.8)\pm0.5$ nm] [5], somewhat closer to the actin filament axis than predicted by either Schutt et al. [3] or Lorenz et al. [6].

Actin has a single high-affinity binding site for either ATP or ADP, and for a bivalent cation. Both ligands are located in the cleft separating the two actin domains [1]. Under physiological conditions Mg^{2+} is the tightly bound cation (for a review, see [7]). However, for technical reasons, the atomic structures of actin have been solved with either Ca^{2+} [1,2] or Sr^{2+} [3] at this site.

The intrinsic fluorescence [8] and NMR spectra [9] both suggest that the conformations of Ca-G-actin and Mg-G-actin are different. The fluorescence intensity of an acetyl-*N*′-(5-sulpho-1-naphthyl)ethylenediamine (AEDANS) label bound to Cys^{374} [8,10–13] or of 7-chloro-4-nitrobenzeno-2-oxa-1,3-diazole attached to Lys^{373} [14], as well as changes in the proteolytic susceptibility of actin [15], suggest that the species of strongly bound cation influences the conformation of the C-terminal segment. Digestion experiments [15] also revealed cation-dependent structural changes in the segment comprising residues 61–69 of subdomain 2. Changes in antigenicity are indicative of cation-induced conformational alterations around Val^{201} in subdomain 4 [16] and in residues 18–29 of subdomain 1 [17].

X-ray diffraction studies of the actin–DNase I complex indicate that the structures of ATP- and ADP-actin are very similar [1]. However, biochemical evidence suggests that this similarity may be imposed by the binding of DNase I. Substitution of ADP for ATP in Mg-G-actin diminishes the fluorescence intensity of AEDANS attached to Cys^{374} [18] and increases the reactivity of Cys^{10} [19]. Limited proteolysis experiments reveal nucleotide-dependent structural changes in the C-terminal segment, in the

Abbreviations used: AEDANS, acetyl-*N*′-(5-sulpho-1-naphthyl)ethylenediamine; DC, dansylcadaverine; DDPM, *N*-[4-(dimethylamino)-3,5-dinitrophenyl]maleimide; DED, dansylethylenediamine; FRET, fluorescence resonance energy transfer.

‡ To whom correspondence should be sent, at Warsaw address.

central segment of the DNase I binding loop, and in the environment of Arg^{62} and Lys^{68} in subdomain 2 [15]. Structural differences between ATP- and ADP-G-actin are also apparent from kinetic parameters of actin polymerization (for a review, see [20]).

Fluorescence resonance energy transfer (FRET) has been widely used to study actin structure (for a review, see [21]). A model of G-actin based on seven different FRET loci agrees well with the atomic structure [22]. Lingering doubts over the importance of κ^2, the orientation factor, have largely been dispelled and the FRET method has emerged as being particularly valuable for detecting small structural changes in proteins that are beyond the current scope of X-ray diffraction and electron microscopy [23].

In this paper we have applied the FRET technique to study the influence of DNase I binding and of the effects of exchanging nucleotide and metal ion ligands on the intramonomer distance between Gln^{41} within the DNase I binding loop of subdomain 2 and Cys^{374} in the C-terminal segment of subdomain 1 of actin. Dansyl cadaverine (DC) enzymically conjugated to Gln^{41} was used as the energy donor, and Cys^{374} was labelled with *N*-[4-(dimethylamino)-3,5-dinitrophenyl]maleimide (DDPM) as the energy acceptor.

MATERIALS AND METHODS

Reagents

DC was purchased from Molecular Probes Inc. DDPM was from Aldrich Chemical Co. Bovine pancreatic DNase I was obtained from Sigma Chemical Co. or from Worthington Biochemicals (#DPRFS, molecular biology grade, protease free). Sephadex G-25 and Sephacryl S-200 were from Amrad Pharmacia Pty Ltd. Guinea pig liver transglutaminase and all other reagents were purchased from Sigma Chemical Co.

Protein preparations

Actin was extracted from acetone-dried powder of rabbit skeletal muscle and was purified as described by Spudich and Watt [24]. Isolated Ca-ATP-G-actin was prepared in 2 mM Tris/HCl, pH 8.0, 0.2 mM ATP, 0.1 mM $CaCl_2$ and 0.02% NaN_3 (G buffer) on ice, and was used within 1 week.

Mg-ATP-G-actin was prepared directly before measurements by incubation of Ca-ATP-G-actin (twice diluted with a Ca^{2+}-free G buffer to decrease the concentration of $CaCl_2$) with 0.2 mM EGTA/0.1 mM $MgCl_2$ for 10–15 min at 20 °C.

Actin with ADP at the nucleotide binding site was produced essentially according to the method described by Gershman et al. [25]. Mg-ATP-G-actin was incubated with hexokinase (10 units/ml) and 0.5 mM glucose at 23 °C. The reaction was monitored by measuring the change in fluorescence of the DC label. The final, constant, value was reached within about 2 h, in good agreement with the kinetics of ATP/ADP exchange reported previously [25]

Truncated actin from which the three C-terminal residues had been removed was obtained by digestion of Mg-ATP-G-actin with trypsin as described by Mossakowska et al. [26]. The reaction was stopped with a 3-fold molar excess of soybean trypsin inhibitor. The actin was then passed through a polymerization/depolymerization cycle followed by overnight dialysis against G buffer.

Before use, actin was clarified by centrifugation for 45 min at 100000 ***g***.

Labelling of actin with DC and DDPM

DC was covalently bound to Gln^{41} essentially as described by Takashi [27]. Actin (3–4 mg/ml) was incubated with guinea pig transglutaminase (0.1 unit/ml) and a 5-fold molar excess of DC in a solution containing 5 mM Tris/HCl, pH 8.0, 1 mM $CaCl_2$, 0.4 mM ATP and 1 mM dithiothreitol. After 20 h at 2 °C, the actin solution was further incubated at room temperature for 5 h. The reaction was terminated by adding EGTA at a final concentration of 1 mM. Actin was then supplemented with 50 mM KCl and 2 mM $MgCl_2$ to ensure complete polymerization, and the polymer was collected by centrifugation at 150000 ***g*** for 1.5 h. F-actin pellets were homogenized in G buffer and exhaustively dialysed against this buffer. Traces of unbound label were removed by passing the actin solution through a Sephadex G-25 column equilibrated with G buffer. The concentration of DC attached to actin was measured spectrophotometrically using a molar absorption coefficient of $4.64 \times 10^3\ M^{-1} \cdot cm^{-1}$ at 326 nm [28]. The labelling ratio of five independent preparations varied between 0.43 and 0.60.

DC-actin was subsequently labelled at Cys^{374} with the non-fluorescent acceptor DDPM, as described by Miki [29]. DC-actin (3–4 mg/ml) in G buffer was supplemented with ATP to a final concentration of 0.5 mM and incubated with a 5-fold molar excess of DDPM at 2 °C. After 20–24 h the reaction was quenched by the addition of β-mercaptoethanol to a final concentration of 1 mM. The modified actin was dialysed against G buffer, clarified by centrifugation at 100000 ***g*** for 45 min and filtered through a Sephadex G-25 column. The labelling ratio was calculated using a molar absorption coefficient of $3.05 \times 10^3\ M^{-1} \cdot cm^{-1}$ at 440 nm [30]. The labelling ratio of five independent preparations was between 0.50 and 0.93.

Gel filtration of labelled actin

Gel filtration of both single- and double-labelled actin was performed on a column of Sephacryl S-200 using G buffer as the eluent.

Determination of protein concentrations

The concentrations of native and C-terminal-truncated actin were measured spectrophotometrically using an absorption coefficient of $0.63\ mg \cdot ml^{-1}$ at 290 nm [31]. The concentration of fluorescently labelled actin was determined by the Bradford method [32] using the Pierce Protein Assay reagent as described by the manufacturer.

DNase I inhibition assay

Inhibition of DNase I activity by G-actin was measured spectrophotometrically [33] as described in [34]. The DNase I concentration in the assay mixture was 5 μM, DNA was present at 100 μg/ml, and the actin concentration was varied between 0.5 and 7.5 μM.

Fluorescence spectroscopy

The steady-state fluorescence intensity was measured in an SLM 8000 photon counting spectrofluorimeter, operated in the ratio mode, or in a Spex Fluorolog spectrofluorimeter (Spex Industries, Edison, NJ, U.S.A.). DC-labelled G-actin was excited at 332 nm.

Emission spectra, both in the presence and in the absence of the acceptor, were recorded over the range 440–600 nm.

Energy transfer from donor to acceptor is reciprocally related to the sixth power of the distance separating the probes [35], by the equation:

$$E = R_o^6/(R_o^6 + R^6) \quad (1)$$

where R_o is Förster critical distance at which transfer efficiency is equal to 50 %, and R is the distance between the donor and acceptor probes. The R_o distance for DC and DDPM as donor–acceptor pair was calculated to be 29 Å (2.9 nm) (T. Tao, unpublished work cited in [21]).

The efficiency of fluorescence resonance energy transfer (E) was determined by measuring the fluorescence intensity of the donor (DC) in both the presence (F_{DA}) and the absence (F_D) of the acceptor, according to the equation:

$$E = (1 - F_{DA}/F_D)/\alpha \quad (2)$$

where α is the degree of the labelling with the acceptor of the double-labelled actin. No correction for non-stoichiometric labelling with the donor was necessary, because donor-free molecules are simply not detected in the fluorescence measurements.

All spectra were recorded at about 1 μM donor concentration. Determination of the degree of DC labelling in double-labelled actin is, however, complicated because of the broad nature of the absorption spectrum for the DDPM acceptor. Another difficulty arises from the fact that the acceptor can diminish the donor fluorescence, not only through resonance energy transfer but also by re-absorption of the excitation and/or emission photons (inner-filter effects). To overcome these difficulties, samples of DC- and DC/DDPM-G-actin were subjected to extensive fragmentation by prolonged trypsin digestion (see below) to separate donor- and acceptor-labelled peptides, thus abolishing the resonance energy transfer. After digestion, the fluorescence of both samples was measured again in the presence of 1 % SDS. The donor fluorescence intensities of intact actin were then normalized according to [36], by multiplying the intensity of DC fluorescence in double-labelled actin (F_{DA}) by the ratio of DC fluorescence in the digests of DC-actin (F'_D) and DC/DDPM-actin (F'_{DA}). Inserting this correction into eqn. (2), we obtain:

$$E = (1 - F_{DA}F'_D/F_DF'_{DA})/\alpha \quad (3)$$

Trypsinolysis of labelled actin

Preparations of DC- and DC/DDPM-labelled Ca-G-actin were digested overnight at 4 °C with trypsin at an enzyme/protein mass ratio of 1:10. The reaction was stopped with soybean trypsin inhibitor in a 4 × molar concentration of trypsin. Actin was hydrolysed into peptides which were too small to be retarded on SDS/PAGE.

RESULTS

Distance separating Gln[41] and Cys[374] in Ca-ATP-G-actin

The maximum of the fluorescence emission of DC-labelled Ca-ATP-actin was at 512 ± 1.6 nm, whereas the peak for free DC in G buffer was at 555 nm. This shift suggests that the fluorophore conjugated to actin interacts with appropriately oriented hydrophobic side chains of the protein moiety which diminishes its exposure to solvent.

The fluorescence intensity of the dansyl probe in DC/DDPM-labelled G-actin was significantly lower than in actin labelled with DC only (Figure 1, curves 1 and 1′), which shows that the probes are located within a sufficiently small distance for fluorescence energy transfer to occur between them. From eqn. (3), the efficiency of energy transfer was calculated to be 0.264 ± 0.040 (mean ± S.D. for six different preparations). With the Förster critical distance (R_o) for the DC/DDPM pair on actin taken as 29 Å (T. Tao, personal communication), a value of 34.4 ± 1.3 Å for the distance between the donor and acceptor pair in Ca-ATP-G-actin was obtained.

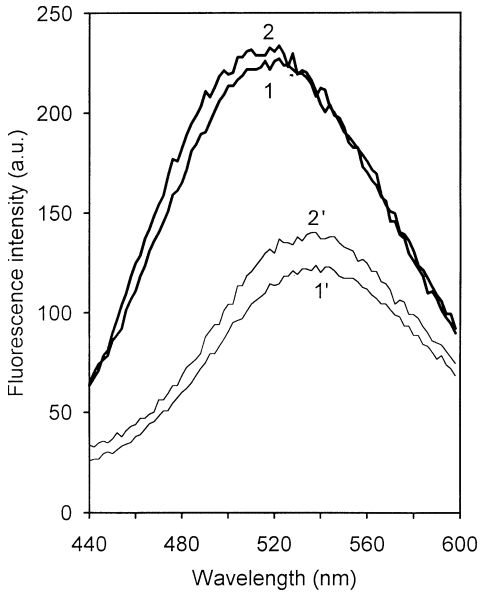

Figure 1 Fluorescence emission spectra of DC-G-actin (curves 1 and 2) and DC/DDPM-G-actin (curves 1′ and 2′) in the absence (curves 1 and 1′) and presence (curves 2 and 2′) of DNase I

The fluorescence intensities of DC- and DC/DDPM-G-actin were normalized to a 1 μM donor concentration. The fluorescence of DC/DDPM-G-actin was also corrected for non-stoichiometric labelling with the acceptor. The measurements were done on 7.1 μM Ca-ATP-G-actin in G buffer at 23 °C. DNase I (dissolved in G buffer) was added in a 1.5-fold molar excess over actin. The excitation wavelength was 332 nm. a.u., arbitrary units.

Influence of DNase I binding on the fluorescence spectra of DC- and DC/DDPM-G-actin

The atomic structure of the actin–DNase I complex has demonstrated that Gln[41] is located in a region of direct contact between the two proteins [1]. Despite this, labelling of actin at Gln[41] with DC did not significantly change the ability of actin to inhibit the DNase I activity. At a 1:1 actin/DNase I molar ratio we observed complete inhibition by both non-labelled and DC-labelled actin (results not shown).

Binding of DNase I to DC-G-actin did not cause a substantial shift in the position of the fluorescence maximum of the label. The quantum yield of the fluorescence increased by about 3 % (Figure 1, curves 1 and 2). The efficiency of FRET in the double-labelled actin decreased upon addition of DNase I from 0.260 to 0.232 only (mean values for two different preparations of Ca-ATP-G-actin).

Earlier measurements by dos Remedios et al. [37] with the same donor/acceptor pair reported that DNase I binding caused a decrease in FRET efficiency, which suggested that there was a significant increase in the inter-probe distance when DNase I binds. This discrepancy has now been resolved by showing that

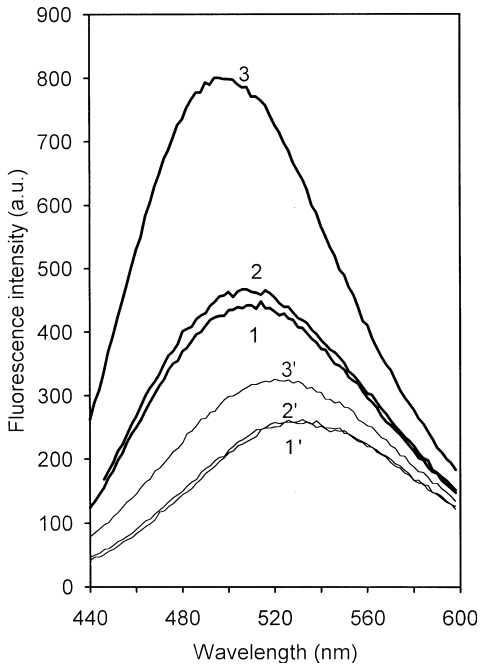

Figure 2 Influence of the type of bivalent cation and nucleotide bound to G-actin on the fluorescence emission spectra of the DC label

Ca-ATP-G-actin, curves 1 and 1′; Mg-ATP-G-actin, curves 2 and 2′; Mg-ADP-G-actin, curves 3 and 3′. Curves 1, 2 and 3 represent DC-labelled actin, and curves 1′, 2′ and 3′ DC/DDPM-labelled actin. The Ca^{2+}/Mg^{2+} and ATP/ADP exchanges were carried out in a fluorescence cuvette as described in the Materials and methods section. All spectra were normalized to a 1 μM donor concentration. The spectra of DC/DDPM-actin were also corrected for non-stoichiometric labelling with the acceptor. a.u., arbitrary units.

a slow but extensive fragmentation of actin is produced by a protease(s) present as a contamination in their [37] DNase I samples (Sigma Chemical Co.), which decreased the fluorescence intensity of the dansyl fluorophore because of its exposure to the polar environment of the solvent. The degradation of actin was eliminated when soybean trypsin inhibitor was added together with Sigma DNase I, and was not observed when a protease-free preparation of DNase I (from Worthington) was used.

Effects of the type of tightly bound cation and nucleotide on the conformation of subdomain 2 in G-actin

Substitution of Mg^{2+} for Ca^{2+} initially bound at the high-affinity site for bivalent cations in DC-actin resulted in an increase of about 5% in the intensity of the DC fluorescence and in a small blue shift of the fluorescence maximum (Figure 2, Table 1). These changes were fairly reproducible, suggesting that replacement of Ca^{2+} by Mg^{2+} causes a small but significant change in the environment of the dansyl fluorophore.

Further and more pronounced changes were observed when the bound ATP in Mg-G-actin was exchanged for ADP (Figure 2, curves 3 and 3′). The fluorescence intensity of DC-labelled Mg-ADP-G-actin was about 70% higher than that of Mg-ATP-G-actin. This nucleotide exchange was also accompanied by a large blue shift of the spectrum (Table 1), consistent with a shift of the fluorophore to more hydrophobic surroundings.

There was a small increase in the energy transfer efficiency from the dansyl fluorophore to the DDPM acceptor in double-labelled actin on replacement of the bound Ca^{2+} with Mg^{2+}, and a further large increase on transformation of Mg-ATP-G-actin into Mg-ADP-G-actin (Table 1). Calculation of the interprobe distance from these data must take into account the concomitant changes in the R_o value. Because of the broad nature of the acceptor absorption spectrum, the shifts of the donor emission maximum resulting from Ca^{2+}/Mg^{2+} and ATP/ADP replacement had a small effect on the donor/acceptor spectral overlap and produced only a 0.1% increase in R_o. Correction for the increase in quantum yield of DC in single-labelled actin led to R_o values of 29.2 Å for Mg-ATP-G-actin and 31.8 Å for Mg-ADP-G-actin. With these values, the distance between the donor and acceptor pair was calculated to be 34.1 ± 1.6 Å in Mg-ATP-G-actin and 35.9 ± 0.5 Å in Mg-ADP-G-actin. The differences between these values and that obtained for Ca-ATP-G-actin are within the scatter of the measurements for each of these preparations.

Table 1 Summary of the observed effects

The procedures for Ca^{2+}/Mg^{2+} and ATP/ADP exchange and for preparation of the C-terminal-truncated actin, as well as the details of the measurements and calculations, are described in the Materials and methods section. The data are means $\pm$ S.D. (wherever appropriate). The numbers of different preparations of labelled actin used in the measurements are given in the parentheses. λ_{max} is the wavelength of the emission maximum of DC label after excitation at 332 nm. F/F_{Ca} is the ratio of the DC fluorescence of a given form of actin to that of Ca-ATP-G-actin. E is the transfer efficiency between the donor (DC) and the acceptor (DDPM). R_o and R are the Förster critical distance and the interprobe FRET distance respectively.

	DC-G-actin		DC/DDPM-G-actin		
Form of actin	λ_{max} (nm)	F/F_{Ca}	E	R_o (Å)	R (Å)
Intact actin					
Ca-ATP (6)	512 ± 1.6	–	0.264 ± 0.040	29.0	34.4 ± 1.3
Mg-ATP (4)	509 ± 2.6	1.05 ± 0.02	0.286 ± 0.062	29.2	34.1 ± 1.6
Mg-ADP (3)	497 ± 4.3	1.71 ± 0.45	0.324 ± 0.021	31.8	35.9 ± 0.5
C-terminal-truncated actin					
Ca-ATP (2)	520	–			
Mg-ATP (2)	516	1.10			
Mg-ADP (2)	498	1.78			

In F-actin, monomers along the long-pitch helix juxtapose Gln^{41} of one monomer very close to Cys^{374} in the suprajacent monomer. Thus the inter-monomer FRET in dimers or short oligomers possibly present in preparations of labelled actin could dominate the distance calculations. Accordingly, a separate set of measurements was performed on DC- and DC/DDPM-actin which were additionally purified by gel filtration on Sephacryl S-200. Although this procedure removed a small amount of some aggregated material migrating in front of the main peak, it did not produce any significant change in the spectral characteristics of the protein preparations. The efficiency of energy transfer for column-purified Ca-ATP-actin was 0.262 ± 0.043 (mean $\pm$ S.D. of six measurements). It increased to 0.283 after substitution of Mg^{2+} for the bound Ca^{2+}, and to 0.342 after subsequent exchange of ATP for ADP. These values are in good agreement with those obtained with non-chromatographed actin (Table 1), showing that the fluorescence changes observed under our experimental conditions are not significantly influenced by intermolecular effects.

In view of the tendency of Mg-actin to form oligomers ([38] and references therein) and of the reported increase in the quantum yield of the fluorescence of the DC label upon actin polymerization [27], we also measured the fluorescence intensities of labelled Mg-ATP-actin as a function of actin concentration. The presence of oligomers that are believed to form above a

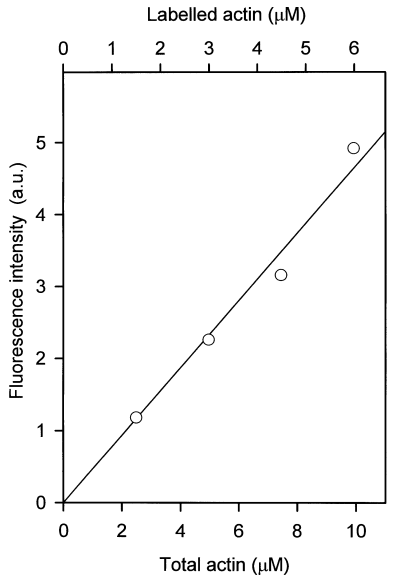

Figure 3 Fluorescence intensity of DC-labelled Mg-ATP-actin as a function of the concentrations of labelled and total actin

The degree of labelling of actin with DC was 0.6. The fluorescence intensity was measured at 512 nm after excitation at 332 nm. a.u., arbitrary units.

certain critical concentration of actin [38] would manifest itself as an increase of the slope of the curves above this concentration. As shown in Figure 3, the fluorescence of DC-actin increased linearly with the concentration of actin at least up to a concentration of 10 μM. Linear plots in this range of protein concentrations were also obtained when the light scattering was measured (results not shown). The results of these control experiments exclude the possibility that the bound Mg^{2+} promoted formation of any significant amount of oligomeric species at the protein concentrations (usually below 2 μM) used in our fluorescence measurements.

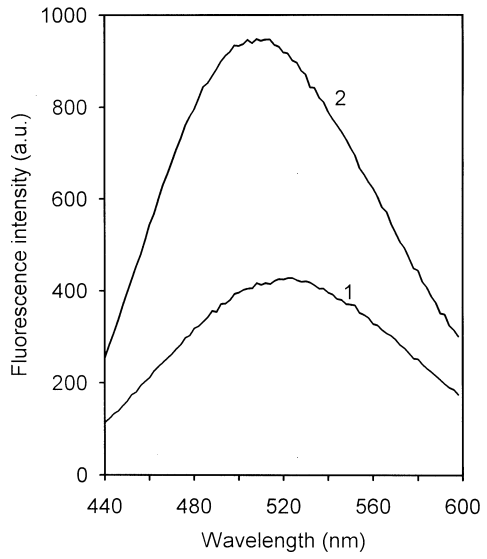

Figure 4 Effect of removal of the three C-terminal residues on the fluorescence emission spectrum of DC attached to Gln^{41} in Ca-ATP-G-actin

The C-terminal-truncated actin was prepared as described in the Materials and methods section. The fluorescence spectra of the DC label in the truncated (curve 1) and unmodified (curve 2) actins were measured in G buffer at 23 °C after adjustment of the concentrations of the two proteins to give the same concentration of label (1 μM). a.u., arbitrary units.

Long-range conformational effects of the removal of the last three residues of G-actin

As shown in Figure 4, proteolytic removal of three amino acid residues from the C-terminus of actin labelled with DC resulted in a more than 2-fold decrease in the fluorescence intensity of the label and in a red shift of the fluorescence spectrum of about 8 nm. Thus removal of residues 373–375 is associated with increased solvation of the DC probe located more than 30 Å away. This modification did not abolish the sensitivity of the fluorescence of the DC probe to the nature of the tightly bound bivalent cation or nucleotide. Exchange of Ca^{2+} for Mg^{2+} and of ATP for ADP in the truncated DC-G-actin produced changes in fluorescence that were essentially the same as those observed with intact DC-actin (Table 1).

DISCUSSION

The glutamine residue at position 41 of the actin sequence is within the polypeptide loop directly involved in DNase I binding to G-actin [1] and, according to the current models of F-actin [6,39], participates in the inter-monomer contacts in the polymer. However, modification of this residue using a bulky moiety such as dansyl neither impairs the actin–DNase I interaction (the present study) nor interferes with the assembly of monomers into filaments [27]. These observations suggest that the probe may be shifted away from the actin–DNase-I/actin–actin contact areas.

The accessibility of Gln^{41} of G-actin to modification by the transglutaminase enzyme suggests that the ϵ-amino group of this residue is exposed to solvent. We observed that the fluorescence emission maximum of DC-actin was blue-shifted by about 43 nm from the peak position of free DC in G buffer. This suggests that the attached dansyl fluorophore resides in a more hydrophobic environment. The dansyl group has a maximum cord of about 7.5 Å, but its effective sphere of influence is increased by the cadaverine [-$(CH_2)_5$-] linker group (7.5 Å). Figure 5(a) shows the α-carbon backbone structure of actin as modelled by Kabsch et al. [1], with those hydrophobic residues that fall within a 15 Å radius of the ϵ-amino group of Gln^{41} shown as space-filled structures (note that this is the rear view of the conventional Kabsch et al. [1] representation, showing subdomains 1 and 2 on the left). This scheme is based on the assumption that the conformation of the DNase I binding loop in free actin in solution is not very different from that in DNase I–actin co-crystals, which seems to be substantiated by our DC fluorescence measurements on free and DNase I-bound actin. As can be seen in Figure 5(a), the possible sphere of influence of the dansyl fluorophore attached to Gln^{41} through the cadaverine chain (assuming that this probe can freely precess) could cover a large area of subdomain 2. Interaction of the fluorophore with the hydrophobic side chains of residues such as Gly^{48}, Pro^{38} and/or Gly^{36} would provide an explanation for the lack of its interference with DNase I binding and actin polymerization, and account for the blue shift in the fluorescence spectrum of the probe on its attachment to actin.

Interaction of the dansyl fluorophore with the side chains of Gly^{36} and/or Pro^{38}, which would bring it closer to the C-terminus of actin, is consistent with the distance of about 34 Å determined from the FRET efficiency between the dansyl donor/DDPM acceptor pair in Ca-ATP-G-actin. This distance is about 10 Å less than the separation between the N^{ϵ} atom of Gln^{41} and

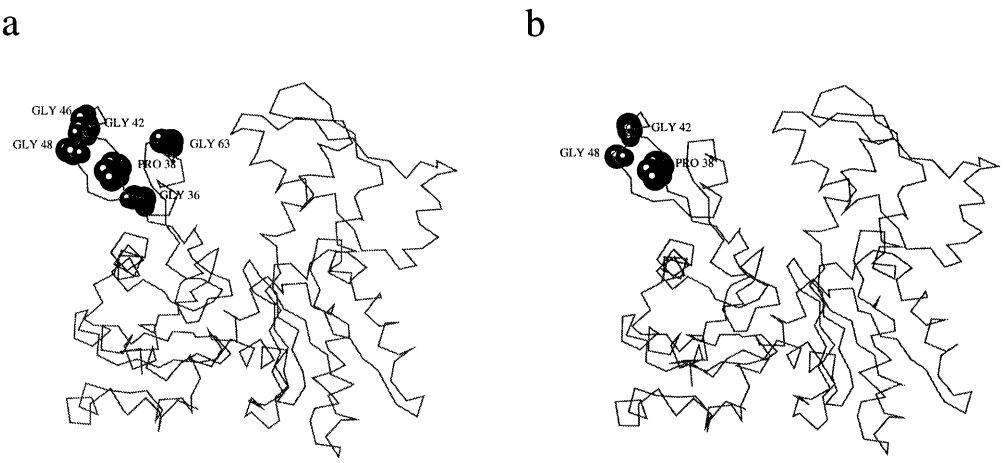

Figure 5 Sphere of influence of the dansyl fluorophore in Ca-ATP-G-actin labelled at Gln^{41} with DC (a) or DED (b)

The actin structure [1] is shown with the small domain (subdomains 1 and 2) on the left and the large domain (subdomains 3 and 4) on the right. Hydrophobic residues which fall within the sphere of influence of the probe are shaded (see text for explanation).

S_γ of Cys^{374} (about 45 Å) calculated from the Kabsch et al. [1] Ca-ATP-G-actin structure with the last three residues from the McLaughlin et al. [2] actin model reconstructed on to it.

The small but significant increase in the fluorescence intensity and the blue shift of the fluorescence maximum of the dansyl fluorophore observed here on substitution of Mg^{2+} for Ca^{2+} bound at the high-affinity site (Table 1) demonstrate that in Mg-ATP-G-actin the fluorophore is in a slightly more hydrophobic environment. Limited proteolysis with a protease from *Escherichia coli* A2 strain which specifically cleaves G-actin between residues 42 and 43 [40], and with subtilisin which cleaves between residues 47 and 48 [41], failed to detect any significant effect of Ca^{2+}/Mg^{2+} replacement on the conformation of the loop comprising residues 38–52 [15]. However, profound changes were detected in the environment of Arg^{62} and Lys^{68} using susceptibility to trypsin as a probe [15]. These observations are in accordance with our suggestion that the location of the dansyl fluorophore is at some distance from the site of its attachment to actin, so that it can detect conformational transitions that do not extend to the DNase I binding loop. The relatively small change in the emission spectrum of the fluorophore on Ca^{2+}/Mg^{2+} replacement in G-actin is consistent with the recently proposed explanation of the cation-dependent changes in G-actin structure in terms of a relative rotation of the two domains which might occur without a substantial structural rearrangement of subdomain 2 [42].

Extensive changes in the conformation of the DNase I binding loop, manifested as a greatly diminished proteolytic susceptibility of peptide bonds 42–43 and 47–48, were observed when the bound ATP in Mg-ATP-G-actin was replaced with ADP [15]. The exact nature of the conformational transitions responsible for this effect could not be evaluated from the proteolysis experiments alone. We have speculated [15] that the DNase I binding loop, protruding from the surface of the molecule in ATP-G-actin, folds back on to subdomain 2 upon replacement of ATP with ADP. This transition would allow for an interaction of its amino acid side chains with residues in the core of subdomain 2, thus diminishing the mobility and, in effect, accessibility of this loop to proteases. A profound structural rearrangement of subdomain 2 associated with transformation of Mg-ATP-G-actin into Mg-ADP-actin is strongly supported by the results of the present study, which show a dramatic increase in the fluorescence intensity of the dansyl fluorophore and a large blue shift in the emission maximum (Table 1). On the other hand, when the increase in the quantum yield of the dansyl fluorophore in Mg-ADP-G-actin is included in the calculation of R_o, there is essentially no change in the FRET distance between the probes on Gln^{41} and Cys^{374}. These results do not, however, preclude a shift in position of the residues of loop 38–52. If this loop moved in a plane perpendicular to the axis between the dansyl and DDPM probes, the change in the inter-probe distance would be negligible.

While this work was being prepared for publication, a related study was published by Kim et al. [43]. These authors measured the fluorescence of actin labelled at Gln^{41} with dansyl ethylenediamine (DED) and an energy transfer between this probe and tryptophan residues in subdomain 1 of actin (principally Trp^{79} and Trp^{86}) as the energy donors. They observed a significant increase in the FRET efficiency on replacement of Ca^{2+} by Mg^{2+} and of ATP by ADP, implying that the distance between the dansyl probe and Trp^{79} and/or Trp^{86} in Mg-ATP-G-actin and Mg-ADP-G-actin may be shorter than in Ca-ATP-G-actin. For the reason outlined above, probes attached to Cys^{374} and Gln^{41} used in our study would fail to detect a movement of loop 38–52 towards Trp^{79} or Trp^{86} if this movement was confined to the surface of a sphere whose centre lies near the 'hinge' region between subdomains 1 and 2.

While the changes in the emission spectrum of DED observed by Kim et al. [43] on going from Ca-ATP-G-actin to Mg-ADP-G-actin are essentially similar to those observed here with DC, a large increase in the fluorescence intensity and blue shift of the fluorescence maximum reported by these authors to occur on replacement of the bound Ca^{2+} with Mg^{2+} in ATP-actin contrast with only small changes observed here. Since their probe (DED) has a shorter linker arm than DC, it is possible that these two probes report changes in the conformation of different areas of subdomain 2. The sphere of influence of the dansyl fluorophore in DED-actin is shown in Figure 5(b) and should be compared with that of the DC probe (Figure 5a). Another contributor to the discrepancy may lie in the different ways of obtaining the Mg-ATP-G-actin. In our experiments the replacement of Ca^{2+} with Mg^{2+} was effected by a short treatment of Ca-ATP-G-actin

with EGTA/$MgCl_2$, whereas the procedure used by Kim et al. [43] involved polymerization of the Mg-ADP form followed by its depolymerization (through dialysis) in the presence of MgATP. In view of slow but significant hydrolysis of ATP on Mg-G-actin [26,38,44] and of the relatively high affinity of MgADP for actin [45], this latter (prolonged) procedure is likely to lead to a mixture of Mg-ATP-G-actin and Mg-ADP-G-actin.

The similarity of the atomic structures of ATP- and ADP-G-actin derived from X-ray diffraction studies of actin complexes with DNase I [1] does not necessarily contradict the nucleotide-dependent change in structure of subdomain 2 of free actin in solution, because DNase I binding across the top of the inter-domain cleft in which the nucleotide binds can be expected to stabilize this part of the actin structure.

Crosbie et al. [46] recently reported the exposure of a new trypsin cleavage site in subdomain 1, near the C-terminus of actin (presumably at Lys^{359}), when DNase I binds. As we show here, the binding of DNase I to actin has little or no effect on the distance between Gln^{41} and Cys^{374} in Ca-ATP-G-actin. This is consistent with the observation [46] that titration with DNase I does not perturb the fluorescence of a pyrenyl label on Cys^{374}, and supports the conclusion that the DNase I-induced perturbation in subdomain 1 does not spread to Cys^{374}. Transmission of structural perturbations in the opposite direction, from the C-terminus to subdomain 2, is apparent from partial exposure to the solvent of the DC label on Gln^{41} upon tryptic removal of the three C-terminal residues of G-actin, which is reflected in the decreased fluorescence intensity and red shift of the emission maximum of the label. This structural alteration in the micro-environment of the fluorophore does not seem to spread to the DNase I binding loop itself, because neither truncation of the C-terminal residues [47] nor placing various probes on Cys^{374} [46] has a significant influence on the proteolytic susceptibility of this loop. Also, inhibition of DNase I activity by G-actin is not altered by the removal of the two or three C-terminal residues [47].

We thank Dr. Wolfgang Kabsch and Dr. Paul McLaughlin for kindly providing the co-ordinates of the atomic structure of the actin molecule. This work was supported by a grant from the National Health & Medical Research Council of Australia, The Ramaciotti Foundations, and by grant 6 P203 011 04 and a grant to the Nencki Institute from the State Committee for Scientific Research (Poland).

REFERENCES

1 Kabsch, W., Mannherz, H. G., Suck, D., Pai, E. F. and Holmes, K. C. (1990) Nature (London) **347**, 37–44
2 McLaughlin, P. J., Gooch, J. T., Mannherz, H. G. and Weeds, A. G. (1993) Nature (London) **364**, 685–692
3 Schutt, C. E., Myslik, J. C., Rozycki, M. D., Goonesekere, N. and Lindberg, U. (1993) Nature (London) **365**, 810–816
4 dos Remedios, C. G. and Moens, P. D. J. (1995) Biochim. Biophys. Acta **1228**, 99–124
5 Moens, P. D. J., Yee, D. and dos Remedios, C. G. (1994) Biochemistry **33**, 3103–3108
6 Lorenz, M., Poole, K. J. V., Popp, D., Rosenbaum, G. and Holmes, K. C. (1995) J. Mol. Biol. **246**, 108–119
7 Estes, J. E., Selden, L. A., Kinosian, H. J. and Gershman, L. C. (1992) J. Muscle Res. Cell Motil. **13**, 272–284
8 Frieden, C., Lieberman, D. and Gilbert, H. R. (1980) J. Biol. Chem. **255**, 8991–8993
9 Barden, J. A. and dos Remedios, C. G. (1985) Eur. J. Biochem. **146**, 5–8
10 Carlier, M.-F., Pantaloni, D. and Korn, E. D. (1986) J. Biol. Chem. **261**, 10778–10784
11 Estes, J. E., Selden, L. A. and Gershman, L. C. (1987) J. Biol. Chem. **262**, 4952–4957
12 Nowak, E., Strzelecka-Gołaszewska, H. and Goody, R. S. (1988) Biochemistry **27**, 1785–1792
13 Valentin-Ranc, C. and Carlier, M.-F. (1989) J. Biol. Chem. **264**, 20871–20880
14 Carlier, M.-F., Pantaloni, D. and Korn, E. D. (1986) J. Biol. Chem. **261**, 10785–10792
15 Strzelecka-Gołaszewska, H., Moraczewska, J., Khaitlina, S. Yu. and Mossakowska, M. (1993) Eur. J. Biochem. **88**, 229–237
16 Mejean, C., Hue, H. K., Pons, F., Roustan, C. and Benyamin, Y. (1988) Biochem. Biophys. Res. Commun. **152**, 368–375
17 Adams, S. B. and Reisler, E. (1994) Biochemistry **33**, 14426–14433
18 Frieden, C. and Patane, K. (1985) Biochemistry **24**, 4192–4196
19 Drewes, G. and Faulstich, H. (1991) J. Biol. Chem. **266**, 5508–5513
20 Carlier, M.-F. (1990) Adv. Biophys. **26**, 51–73
21 Miki, M., O'Donoghue, S. I. and dos Remedios, C. G. (1992) J. Muscle Res. Cell Motil. **13**, 132–145
22 O'Donoghue, S. I., Hambly, B. D. and dos Remedios, C. G. (1992) Eur. J. Biochem. **205**, 591–601
23 dos Remedios, C. G. and Moens, P. D. J. (1995) J. Struct. Biol. **115**, 175–185
24 Spudich, J. A. and Watt, S. (1971) J. Biol. Chem. **246**, 4866–4871
25 Gershman, L. C., Selden, L. A., Kinosian, H. J. and Estes, J. E. (1989) Biochim. Biophys. Acta **995**, 109–115
26 Mossakowska, M., Moraczewska, J., Khaitlina, S. Yu. and Strzelecka-Gołaszewska, H. (1993) Biochem. J. **289**, 897–902
27 Takashi, R. (1988) Biochemistry **27**, 938–943
28 Lorand, J., Rule, N. G., Ong, H. H., Furlanetto, R., Jacobsen, A., Downey, J., Oner, N. and Bruner-Lorand, J. (1968) Biochemistry **7**, 1214–1223
29 Miki, M. (1991) Biochemistry **30**, 10878–10884
30 Gold, A. H. and Segel, H. L. (1964) Biochemistry **3**, 778–782
31 Houk, W. T. and Ue, K. (1974) Anal. Biochem. **62**, 66–74
32 Bradford, M. M. (1975) Anal. Biochem. **72**, 248–254
33 Lindberg, U. (1964) Biochim. Biophys. Acta **82**, 237–248
34 Khaitlina, S. Yu., Moraczewska, J. and Strzelecka-Gołaszewska, H. (1993) Eur. J. Biochem. **218**, 911–920
35 Förster, T. (1948) Ann. Phys. **9**, 21–33
36 Epe, B., Steinhäuser, G. and Woolley, P. (1983) Proc. Natl. Acad. Sci. U.S.A. **80**, 2579–2583
37 dos Remedios, C. G., Kiessling, P. C. and Hambly, B. D. (1994) in Synchrotron Radiation in the Biosciences (Chance, B., Deisenhofer, J., Ebashi, S., Goodhead, D. T., Helliwell, J. R., Huxley, H. E., Iizuka, T., Kirz, J., Mitsui, T., Rubenstein, E. et al., eds.), pp. 418–425, Oxford University Press, Oxford
38 Attri, A. K., Lewis, M. S. and Korn, E. D. (1991) J. Biol. Chem. **266**, 6815–6824
39 Tirion, M. M., Ben-Avraham, D., Lorenz, M. and Holmes, K. C. (1995) Biophys. J. **68**, 5–12
40 Khaitlina, S. Yu., Collins, J. H., Kuznetsova, I. M., Pershina, V. P., Synakevich, I. G., Turoverov, K. K. and Usmanova, A. M. (1991) FEBS Lett. **279**, 49–51
41 Schwyter, D., Philips, M. and Reisler, E. (1989) Biochemistry **28**, 5889–5895
42 Strzelecka-Gołaszewska, H., Woźniak, A., Hult, T. and Lindberg, U. (1996) Biochem. J. **316**, 713–721
43 Kim, E., Motoki, M., Seguro, K., Muhlrad, A. and Reisler, E. (1995) Biophys. J. **69**, 2024–2032
44 Brenner, S. L. and Korn, E. D. (1991) J. Biol. Chem. **256**, 8663–8670
45 Kinosian, H. J., Selden, L. A., Estes, J. E. and Gershman, L. C. (1993) J. Biol. Chem. **268**, 8683–8691
46 Crosbie, R. H., Miller, C., Cheung, P., Goodnight, T., Muhlrad, A. and Reisler, E. (1994) Biophys. J. **67**, 1957–1964
47 Strzelecka-Gołaszewska, H., Mossakowska, M., Woźniak, A., Moraczewska, J. and Nakayama, H. (1995) Biochem. J. **307**, 527–534

Received 20 November 1995/14 March 1996; accepted 27 March 1996